

Title	High-Performance Nonvolatile Write-Once-Read-Many-Times Memory Devices with ZnO Nanoparticles Embedded in Polymethylmethacrylate
Author(s)	Dao, Toan Thanh; Tran, Thu Viet; Higashimine, Koichi; Okada, Hiromasa; Mott, Derrick; Maenosono, Shinya; Murata, Hideyuki
Citation	Applied Physics Letters, 99(23): 233303-1-233303-3
Issue Date	2011-12-06
Type	Journal Article
Text version	publisher
URL	http://hdl.handle.net/10119/10733
Rights	Copyright 2011 American Institute of Physics. This article may be downloaded for personal use only. Any other use requires prior permission of the author and the American Institute of Physics. The following article appeared in Toan Thanh Dao, Thu Viet Tran, Koichi Higashimine, Hiromasa Okada, Derrick Mott, Shinya Maenosono, and Hideyuki Murata, Applied Physics Letters, 99(23), 233303 (2011) and may be found at http://dx.doi.org/10.1063/1.3665937
Description	

High-performance nonvolatile write-once-read-many-times memory devices with ZnO nanoparticles embedded in polymethylmethacrylate

Toan Thanh Dao, Thu Viet Tran, Koichi Higashimine, Hiromasa Okada, Derrick Mott et al.

Citation: *Appl. Phys. Lett.* **99**, 233303 (2011); doi: 10.1063/1.3665937

View online: <http://dx.doi.org/10.1063/1.3665937>

View Table of Contents: <http://apl.aip.org/resource/1/APPLAB/v99/i23>

Published by the [American Institute of Physics](#).

Related Articles

High-performance nonvolatile write-once-read-many-times memory devices with ZnO nanoparticles embedded in polymethylmethacrylate

APL: Org. Electron. Photonics **4**, 265 (2011)

Electrical characteristics and operating mechanisms of nonvolatile memory devices fabricated utilizing core-shell CuInS₂-ZnS quantum dots embedded in a poly(methyl methacrylate) layer

APL: Org. Electron. Photonics **4**, 247 (2011)

Electrical characteristics and operating mechanisms of nonvolatile memory devices fabricated utilizing core-shell CuInS₂-ZnS quantum dots embedded in a poly(methyl methacrylate) layer

Appl. Phys. Lett. **99**, 193302 (2011)

Flexible organic bistable devices based on [6,6]-phenyl-C85 butyric acid methyl ester clusters embedded in a polymethyl methacrylate layer

APL: Org. Electron. Photonics **4**, 236 (2011)

Flexible organic bistable devices based on [6,6]-phenyl-C85 butyric acid methyl ester clusters embedded in a polymethyl methacrylate layer

Appl. Phys. Lett. **99**, 183301 (2011)

Additional information on *Appl. Phys. Lett.*

Journal Homepage: <http://apl.aip.org/>

Journal Information: http://apl.aip.org/about/about_the_journal

Top downloads: http://apl.aip.org/features/most_downloaded

Information for Authors: <http://apl.aip.org/authors>

ADVERTISEMENT

**AIP**Advances

Submit Now

**Explore AIP's new
open-access journal**

- **Article-level metrics
now available**
- **Join the conversation!
Rate & comment on articles**

High-performance nonvolatile write-once-read-many-times memory devices with ZnO nanoparticles embedded in polymethylmethacrylate

Toan Thanh Dao,^{1,2} Thu Viet Tran,^{1,3} Koichi Higashimine,¹ Hiromasa Okada,⁴ Derrick Mott,¹ Shinya Maenosono,^{1,a)} and Hideyuki Murata^{1,a)}

¹Japan Advanced Institute of Science and Technology, 1-1 Asahidai, Nomi, Ishikawa 923-1292, Japan

²University of Transport and Communications, Dong Da, Hanoi, Vietnam

³Le Quy Don Technical University, 100 Hoang Quoc Viet, Cau Giay, Hanoi, Vietnam

⁴International Test & Engineering Services Co., Ltd., 800 Ichimiyake, Yasu, Shiga 520-2392, Japan

(Received 29 October 2011; accepted 10 November 2011; published online 6 December 2011)

A mixture of ZnO nanoparticles and polymethylmethacrylate was used as an active layer in a nonvolatile resistive memory device. Current-voltage characteristics of the device showed nonvolatile write-once-read-many-times memory behavior with a switching time on the order of μs . The device exhibited an on/off ratio of 10^4 , retention time of $>10^5$ s, and number of readout of $>4 \times 10^4$ times under a read voltage of 0.5 V. The emission, cross-sectional high-resolution transmission electron microscopy (TEM), scanning TEM-high angle annular dark field imaging, and energy dispersive x-ray spectroscopy elemental mapping measurements suggest that the electrical switching originates from the formation of conduction paths. © 2011 American Institute of Physics. [doi:10.1063/1.3665937]

Organic nonvolatile resistive memory has emerged as a promising candidate for next-generation memory devices,¹ thanks to its exceptional advantages including fast transition time, solution processability, low temperature processes, and low manufacturing cost.^{1–11} Structurally, an active layer formed by organic material or a compound of polymer and nanoclusters is sandwiched between two electrodes.^{2,3} The two levels of different conductivities of devices can be switched under suitable voltages, enabling the ability to code digital values. Depending on the reproducibility of switching, the resistive memory can be classified into rewritable and write-once-read-many-times (WORM) types.³ For the purpose of data storage archiving, a high-performance WORM resistive memory device is absolutely imperative.^{4–6} WORM memory devices using nanocomposites in which organic molecules^{4,5} or nanoparticles (NPs)⁶ are dispersed phases have been demonstrated. Recently, various types of memory devices with ZnO nanostructures embedded in a polymer matrix have been demonstrated.^{7–11} However, each ZnO-based memory device is reported to be different in type of switching even when made from the same materials. For example, rewritable memory devices have been fabricated using ZnO NPs (Ref. 8) or nanorods⁹ embedded in polymethylmethacrylate (PMMA). ZnO NPs embedded in polystyrene (PS) resulted in rewritable¹⁰ or WORM (Ref. 11) memory devices. Unfortunately, the factors causing the bistability of ZnO-based memory devices are still unclear.^{8,11} Even though ZnO-based WORM memory has achieved up to an on/off ratio of 10^3 ,¹¹ the higher on/off ratio is desired for practical applications.¹² The important characteristics including number of readout and switching time have not been addressed yet.¹¹ Moreover, there is still a lack of evidence to clarify the origins of memory effects.^{7–11}

In this letter, we present an excellent WORM memory device made from ZnO NPs embedded in PMMA. The de-

vice exhibited an on/off ratio of 10^4 , switching time of 1 μs , retention time of $>10^5$ s, and number of readout of $>4 \times 10^4$ times. The on/off ratio was strongly dependent on the weight ratio of ZnO NPs to PMMA. By analyzing with an emission microscope under bias, we concluded the conduction paths (CP) in the device were responsible for the memory effect. Formation of the CPs was further identified through cross-sectional high-resolution transmission electron microscopy (HRTEM), scanning TEM-high angle annular dark field (STEM-HAADF) images, and energy dispersive x-ray spectroscopy (EDS) elemental maps of the device.

Figure 1(a) shows the device structure of the resistive memory. Monodispersed ZnO NPs of mean size of 9.2 ± 1.4 nm were chemically synthesized using our own method¹³ with some modifications.¹⁴ The as-synthesized ZnO NPs were dispersed in a chloroform/n-butylamine mixture. Separately, PMMA (molecular weight 94 600) was dissolved in chloroform. Then, both materials were mixed together at different weight ratios. The ZnO/PMMA dispersion solution

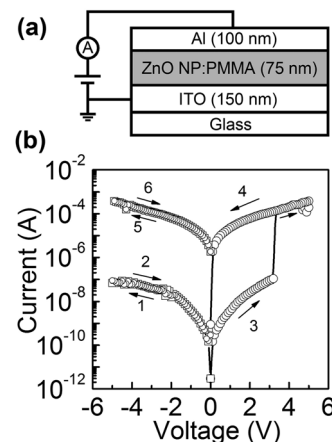


FIG. 1. (a) Device structure and (b) I - V curve of resistive memory device. Arrows indicate bias sweeping direction.

^{a)}Electronic addresses: shinya@jaist.ac.jp and murata-h@jaist.ac.jp.

was spin coated onto a pre-cleaned 150-nm-thick ITO cathode and heated at 100 °C for 80 min in air to form a 75-nm-thick ZnO:PMMA composite layer. Finally, a 100-nm-thick Al anode was thermally deposited on the ZnO:PMMA layer at a base pressure of 7×10^{-6} Torr through a shadow mask (device area 3.5 mm²). The electrical characteristics of the devices were measured with a Keithley 4200 semiconductor characterization system and a Keithley 3390 pulse generator in a dry nitrogen atmosphere at room temperature.

The current-voltage (I - V) curve of the particular memory device with a ZnO:PMMA weight ratio (x) of 1.25×10^{-2} is shown in Fig. 1(b). The device initially exhibited low conductivity state (OFF state). The OFF state was maintained under negative bias (regions 1 and 2). When positive bias was applied (region 3), the OFF state was maintained below 3.2 V, and then, the current abruptly increased at a threshold voltage, $V_{th} = 3.2$ V, changing to high conductivity state (ON state). Once the transition from OFF to ON state took place, the device did not return to the OFF state again even when negative bias was applied (regions 4, 5, and 6) indicating that the switching property of the device is WORM. The on/off ratio was found to be 10^4 at an applied voltage of 0.5 V which is one order of magnitude larger than that of the previously reported ZnO-based WORM device.¹¹

It is well known that PMMA acts as an insulator material.¹⁵ Therefore, the I - V characteristics of the device would be dominated by the size and the number density of ZnO NPs. Indeed, ON and OFF currents and on/off ratio strongly depend on the weight ratio (x) of ZnO NPs to PMMA as shown in Fig. 2, where we plotted the results of three devices having the same value of x . Note here that the data points in Fig. 2 are average values with standard deviations. In all cases, the devices exhibited only WORM characteristics in the range of $10^{-4} \leq x \leq 2 \times 10^{-1}$. The maximum on/off ratio of 10^4 was obtained at $x = 1.25 \times 10^{-2}$. In the case of $x < 10^{-4}$, the device had low conductivity and showed no memory effect. On the contrary, the device exhibited high conductivity state with no memory effect with $x > 2 \times 10^{-1}$.

In practical terms, the retention time is one of the most important characteristics of a memory device. Figure 3(a) shows the retention characteristics of the device ($x = 1.25 \times 10^{-2}$). The OFF state current measurement was firstly carried out at a voltage of 0.5 V. Then, a pulsed positive bias (4 V, 1 μ s) was applied to change the device to ON state followed by the ON current measurement at 0.5 V. The on/off ratio remained unchanged after 10^5 s which is as long as that for

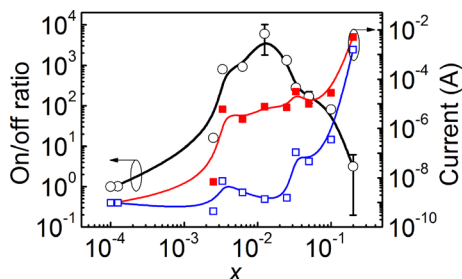


FIG. 2. (Color online) Dependence of OFF current (open square), ON currents (filled square) and on/off ratio (open cycles) on x . Read voltage was 0.5 V.

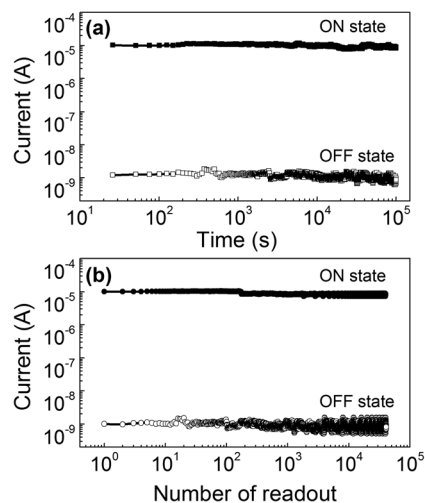


FIG. 3. (a) Retention time characteristics of device. OFF state (initial state) and ON state were continuously measured at bias of 0.5 V (interval 25 s). (b) Number of readout properties of ON and OFF states measured by applying a pulsed bias of 0.5 V (interval 1 μ s).

the ZnO-based memory devices reported previously.^{8,10,11} To investigate the number of readouts, a pulsed positive bias (0.5 V, interval 1 μ s) was applied. Remarkably, ON and OFF currents showed negligible degradation even after 4×10^4 times of data reading.

The charge trapping^{2,8} or CP (Refs. 5 and 16) is the proposed operational mechanism of resistive memories. Several methods were used to investigate CP such as changing the area of the devices,¹⁶ heat-sensitive camera,¹⁷ or the optical beam induced resistance change (OBIRCH).¹⁸ To clarify the mechanism, we first observed the emission of the device during changing the applied voltages by using an EX02 Functional Characteristics emission microscope.¹⁴ The details of this technique are reported elsewhere.¹⁹ When the applied voltage was less than the V_{th} , no visible emission appeared

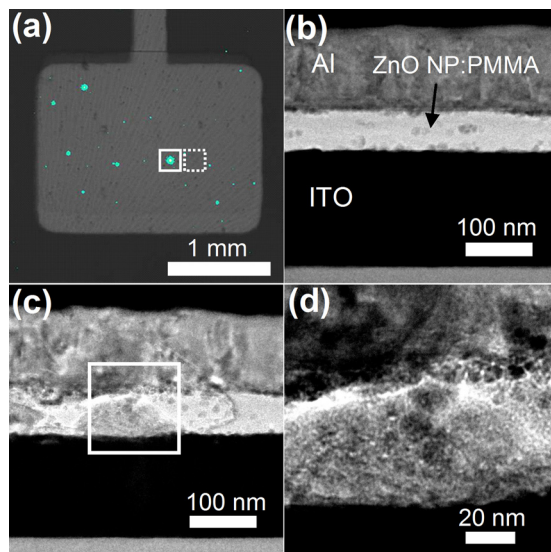


FIG. 4. (Color online) Evidence of CP existence in a WORM memory device. Emission image of device in ON state (a). Cross-sectional HRTEM images of no emission (b) and emission (c) points, and (d) enlarged image of square area in (c). Note that the color of the emission points does not represent the actual emission color and is used for enhancing visibility.

(Fig. S2(a)). The visibly bright spots were observed at a voltage larger than V_{th} with high intensity as shown in Fig. 4(a). And then, when the voltage was reduced again to 3 V, the visible spots remained at the same places but with lower emission intensity (Fig. S2(c)). This phenomenon is consistent with nonvolatile behavior investigated by electrical measurements. The bright spots suggest that the CPs are formed in these places.^{17,19} The origin of the emission could be due to the electroluminescence from the ZnO NPs (Ref. 20) in the CPs. In order to investigate the formation mechanism of the CP, cross-sectional HRTEM and STEM-HAADF imaging and EDS elemental mapping analyses were carried out.¹⁴ Figs. 4(b) and 4(c) show the HRTEM images taken from the cross sections of the selected dark area and bright emission point in Fig. 4(a), respectively. At no emission area, ZnO NPs were found to be uniformly dispersed in PMMA. In contrast, the aggregation of ZnO NPs was observed at the emission point. The enlarged image of the red square part of Fig. 4(c) suggests that there was a conductive channel formed by an aggregation of ZnO NPs (Fig. 4(d)). The STEM-HAADF imaging and EDS elemental mapping of the emission point further confirmed that closely packed ZnO NPs are present across the film.¹⁴ These analyses of the film prove that CPs are formed in our device. The existence of the CPs also agrees well with the relationship of current and x (Fig. 2). The currents tended to increase with increasing the concentration of ZnO NPs. When $x > 2 \times 10^{-1}$, the devices were immediately short-circuited after fabrication owing to the fact that the active layer is mainly NPs, resulting in very large currents. But, when $x < 10^{-4}$, CPs could not be generated due to the negligible appearance of ZnO NPs in PMMA, causing the currents to be very low.

The formation of CPs was in association with the conductive NPs bridging the two electrodes after the application of voltage over V_{th} . For instance, there were some places where the NPs were aggregated in the film after spin-coating (Figs. 4(c) and 4(d)). Under electric fields, electrons were injected from ITO (the work function of ITO = 4.6 eV (Ref. 21)) to the ZnO NPs (electron affinity = 4.4 eV (Ref. 10)) and acted as an extension of the ITO electrode.¹⁶ The NPs contacting the ITO electrode could connect to a neighboring NP. The electric fields between the neighboring NPs increase with increasing the applied voltages. At the applied voltage of V_{th} , the CPs formed through the conductive NPs bridging with the ITO and Al electrodes. Once the CP forms, the resistance of the CP is lower than that of other places so that the current always paths through at the CP. This phenomenon results in the observed WORM behavior.

To check the reproducibility of V_{th} in WORM memory devices, we characterized a total number of 136 devices where 132 of them switched to the ON state at positive bias and only 4 devices turn to ON state at negative bias.¹⁴ The reasons for the domination of positive operation could be due to the stronger interaction between ZnO NPs and the

ITO surface. Namely, the smaller surface energy difference between ZnO NPs and ITO rather than the air side is favorable to condense ZnO NPs at the ITO surface during the spin-coating of the ZnO NPs:PMMA film or during heating of the film.

In summary, a high-performance WORM memory device was fabricated by using ZnO NPs:PMMA nanocomposite sandwiched between ITO and Al electrodes. The memory effect is attributed to the CP formation. The device showed a maximum on/off ratio of 10^4 . The transition from OFF to ON state can take place with a pulse width of 1 μ s. The WORM memory devices can be reproducibly fabricated and they show high stability.

This work was partially supported by a Grant-in-Aid Grant No. 20241034 and Scientific Research on Innovative Areas “ π -Space” Grant No. 20108012 from the Ministry of Education, Culture, Sports, Science, and Technology, Japan. D.T.T. and T.V.T. gratefully acknowledge financial support by 322 Scholarships (doctoral course) of the Vietnamese Government.

¹J. J. Kim, B. Cho, K. S. Kim, T. Lee, and G. Y. Jung, *Adv. Mater.* **23**, 2104 (2011).

²J. C. Scott and L. D. Bozano, *Adv. Mater.* **19**, 1452 (2007).

³D. Prime and S. Paul, *Philos. Trans. R. Soc. London, Ser. A* **367**, 4141 (2009).

⁴Y. Ji, S. Lee, B. Cho, S. Song, and T. Lee, *ACS Nano* **5**, 5995 (2011).

⁵M. A. Mamo, W. S. Machado, W. A. L. van Otterlo, and N. J. Coville, *Org. Electron.* **11**, 1858 (2010).

⁶J. Leppaniemi, M. Aronniemi, T. Mattila, A. Alastalo, M. Allen, and H. Seppa, *IEEE Trans. Electron Devices* **58**, 151 (2011).

⁷K. H. Park, J. H. Jung, F. Li, D. I. Son, and T. W. Kim, *Appl. Phys. Lett.* **93**, 123104 (2008).

⁸D. I. Son, C. H. You, W. T. Kim, J. H. Jung, and T. W. Kim, *Appl. Phys. Lett.* **94**, 132103 (2009).

⁹Z. L. Tseng, P. C. Kao, M. F. Shih, H. H. Huang, J. Y. Wang, and S. Y. Chu, *Appl. Phys. Lett.* **97**, 212103 (2010).

¹⁰F. Verbakel, S. C. J. Meskers, and R. A. J. Janssen, *J. Appl. Phys.* **102**, 083701 (2007).

¹¹D. Y. Yun, J. K. Kwak, J. H. Jung, T. W. Kim, and D. I. Son, *Appl. Phys. Lett.* **95**, 143301 (2009).

¹²H. Zhang, L. Liu, B. Gao, Y. Qiu, Z. Liu, J. Lu, R. Han, J. Kang, and B. Yu, *Appl. Phys. Lett.* **98**, 042105 (2011).

¹³T. V. Thu and S. Maenosono, *J. Appl. Phys.* **107**, 014308 (2010).

¹⁴See supplementary material at <http://dx.doi.org/10.1063/1.3665937> for ZnO NP synthesis, emission image microscopy, cross-sectional TEM measurement method, STEM-HAADF images EDS data, and a histogram of V_{th} .

¹⁵T.-S. Huang, Y.-K. Su, and P.-C. Wang, *Appl. Phys. Lett.* **91**, 092116 (2007).

¹⁶B. Cho, T.-W. Kim, M. Choe, G. Wang, S. Song, and T. Lee, *Org. Electron.* **10**, 473 (2009).

¹⁷M. Colle, M. Buchel, and D. M. de Leeuw, *Org. Electron.* **7**, 305 (2006).

¹⁸H.-T. Lin, C.-Y. Lin, Z. Pei, J.-R. Chen, Y.-J. Chan, Y.-H. Yeh, and C.-C. Wu, *Org. Electron.* **12**, 1632 (2011).

¹⁹Y. Luo and N. Miura, in Proc. ASID 2004: Proceedings of the 8th Asian Symposium on Information Display, Nanjing, China, Society for Information Display, USA, February 15-17, 2004, pp. 485-488.

²⁰C.-Y. Lee, Y.-T. Haung, W.-F. Su, and C.-F. Lin, *Appl. Phys. Lett.* **89**, 231116 (2009).

²¹Y. Kinoshita, T. Hasobe, and H. Murata, *Appl. Phys. Lett.* **91**, 083518 (2007).